

Changes in Oligonucleotide Conformation on Nanoparticle Surfaces by Modification with Mercaptohexanol

Sunho Park,[†] Katherine A. Brown,[‡] and Kimberly Hamad-Schifferli^{*†‡}

Department of Mechanical Engineering and Biological Engineering Division,
Massachusetts Institute of Technology, 77 Massachusetts Avenue,
Cambridge, Massachusetts 02139

Received July 8, 2004; Revised Manuscript Received August 16, 2004

ABSTRACT

The conformation of thiol-linked oligonucleotides on the surface of Au nanoparticles was controlled by treatment with 6-mercapto-1-hexanol (MCH). MCH displaces noncovalent base adsorption to the surface, changing the oligo conformation on the Au surface. By controlling MCH concentration and reaction time, a change in effective size (D_{eff}) of the Au–DNA conjugates and improved hybridization ability was observed, suggesting a reduced nonspecific adsorption of the oligo to the Au.

Nanoparticle labeling of DNA oligonucleotides has many applications in sensing, programmable assembly of nanostructures, and control.^{1–5} The linking of nanoparticles to oligos is most commonly achieved by a thiol on the 5' or 3' end of the oligo, leaving the bases unobstructed for hybridization to its complement. However, oligos tend to adsorb to Au surfaces through the nucleotides, inhibiting hybridization by preventing base pairing. Nucleotide adsorption has been determined to depend on oligonucleotide content, oligo length, and coverage.^{6,7} This is an important issue in microarrays, self-assembly of DNA nanostructures, nanoparticle sensors of DNA targets,⁸ and nanoparticle control of DNA hybridization,⁴ where proper hybridization is necessary for function.^{9–14} Therefore, it would be advantageous to have a way to chemically destabilize nucleotide adsorption so that constraints on sequence and length do not necessarily limit hybridization ability.

Different methods for preventing DNA surface adsorption have been explored, such as electric fields¹⁵ and chemical treatment, which orient the DNA perpendicularly and facilitate hybridization. 6-Mercapto-1-hexanol (MCH) has been used previously as an Au passivating species on 2D surfaces and large nanostructures. It displaces the noncovalent and nonspecific adsorption of thiolated DNA, improving hybridization to complementary strands.^{16,17} This molecule takes advantage of the stabilization of self-assembled monolayers (SAMs) by matching the C6 of the thiol group on the 5' end of the DNA that is inherently incorporated in

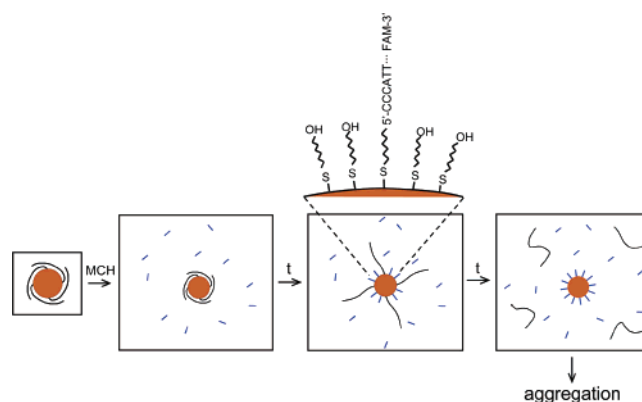


Figure 1. Schematic of the effect of MCH treatment (blue) on DNA–nanoparticle conjugates. MCH prevents nucleotide adsorption, resulting in a more radial configuration of the DNA. Longer reaction times result in total displacement of the DNA from the nanoparticle surface, and eventually aggregation.

synthesis. Here we use chemical modification of the Au nanoparticle surfaces with MCH to control the conformation of the oligo (Figure 1). A conformational change is measured by gel electrophoresis, and enhanced hybridization capacity is confirmed. We find that controlling the reaction time and MCH concentration is key, as thiols have been used to completely displace the DNA from the nanoparticle as a means of quantifying DNA coverage.¹⁸

Au nanoparticles with mean diameters 9.4 nm were obtained commercially (Ted Pella). They were functionalized with the ligand BPS (bis(*p*-sulfonatophenyl) phenylphosphine dihydrate, dipotassium salt) and covalently linked to 15mers of thiolated, single-stranded DNA (DNA-SH, sequences in

* Corresponding author. E-mail: schiffer@mit.edu.

[†] Department of Mechanical Engineering.

[‡] Biological Engineering Division.

Table 1. Sequence of DNA Oligonucleotides

| | |
|-----------------------------|-----------------------------|
| thiolated oligo (DNA-SH) | 5'HS-CCCATTGTGGATTAG-FAM 3' |
| complementary oligo (DNA-c) | 5'TAMRA-CTAATCCACAATGGG-3' |

Table 1) by literature methods.¹⁹ Au–DNA conjugates were purified by gel electrophoresis and resuspended in $0.5\times$ TBE.

The Au–DNA conjugates at $0.1\ \mu\text{M}$ were exposed to MCH in water at concentrations from $1\ \mu\text{M}$ to $1\ \text{mM}$, with reaction times from 1 min to 10 min. Reactions were halted by three washes with $3\times$ volume of ethyl acetate, which extracts excess MCH out of the aqueous solution. MCH extraction is crucial as it permits control of reaction time, which is essential for avoiding complete displacement of the oligo and ligand. This loss of charge leads to nanoparticle aggregation (Figure 1). In contrast to 2D surfaces and large nanoparticle suspensions, the Au–DNA conjugates are soluble and thus the MCH cannot be simply washed away.

Au:DNA ratios were quantified after MCH treatment. Previously, mercaptoethanol has been used to completely displace the DNA oligos to allow quantification of surface coverage of the nanoparticles by fluorescence spectroscopy.¹⁸ Here we used excess MCH for long reaction times and high concentrations to quantify the Au:DNA ratios by total displacement. Samples were extracted from agarose gels and exposed to MCH at $1\ \text{mM}$ for at least 24 h. Au nanoparticles were removed by centrifugation. Before centrifugation, gold nanoparticle concentrations were measured by optical absorption (via Au plasmon peak, $\epsilon\sim 8.5\times 10^7\ \text{M}^{-1}\ \text{cm}^{-1}$). Discarded oligos were quantified by fluorescence (via FAM) spectroscopy.

MCH reaction gives rise to a change in the conformation of the DNA-SH on the nanoparticle surface and presumably results in a change in the effective size (D_{eff}) of the sample. Gel electrophoresis is a technique sensitive to DNA conformation in Au–DNA conjugates.^{7,19,20} Figure 2a shows a 3% gel containing Au–DNA ($\sim 1:3.7$ coverage ratio) samples that have been exposed to various MCH conditions. The bands have a slightly lower mobility compared to Au–DNA (lane 2) with MCH treatment at low concentrations (lanes 3–6). However, samples that have been exposed to MCH at high concentration ($\geq 0.1\ \text{mM}$, lanes 7–9) have a mobility that is higher than Au–DNA, which suggests that reaction with concentrated MCH displaces the oligo from the nanoparticle surface.

To quantify the change in D_{eff} with MCH treatment, gel shifts were evaluated by the Ferguson plot method. Band migration distances were measured by digital image capture, and the position of the band was determined by line scans down the center of the lanes in the image and converted to an absolute mobility, M ($M = \text{velocity}/\text{field strength}$). Figure 2c shows a Ferguson plot generated by collecting the mobility of gel percentage, T (w/v). As control experiments, MCH was treated on plain Au particles. To obtain a value for D_{eff} ,

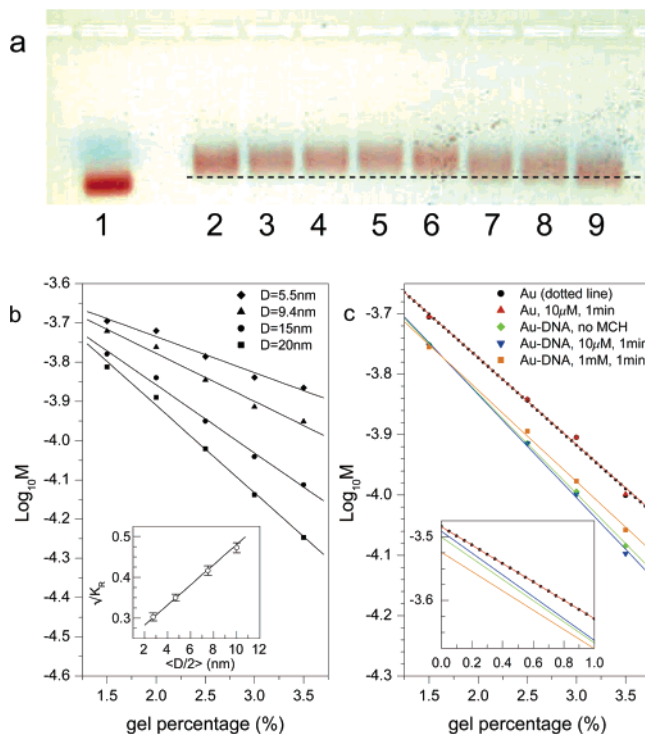


Figure 2. (a) Gel electrophoresis of Au–DNA in a 3% agarose gel of 9.4 nm diameter Au with a coverage ratio of 1:3.7 Au/DNA. The dashed line is a guide for the eye. Lanes: (1) Au, (2) Au–DNA, (3) Au–DNA with $1\ \mu\text{M}$ MCH treatment for 1 min, (4) $1\ \mu\text{M}$ 10 min, (5) $10\ \mu\text{M}$ 1 min, (6) $10\ \mu\text{M}$ 10 min, (7) $0.1\ \text{mM}$ 1 min, (8) $0.1\ \text{mM}$ 10 min, (9) $1\ \text{mM}$ 1 min. (b) Ferguson analysis. $\text{Log}_{10}M$ as a function of gel percentage for calibration standards of Au nanoparticles of mean size of 5.5 nm (diamonds), 9.4 nm (triangles), 15 nm (circles), and 20 nm (squares). M is the mobility of each sample in [cm^2/Vs]. The data are fit to a linear model based on the K_R . Inset: $\sqrt{K_R}$ vs radius fit to a linear regression. (c) $\text{Log}_{10}M$ vs gel percentage for Au and Au–DNA (9.4 nm/1:3.7) with different MCH treatments. Inset: enlargement of low gel percentage region ($<1\%$).

$\text{Log}_{10}M$ is plotted as a function of T , and is fit according to the linear equation:²¹

$$\text{Log}_{10}M = \text{Log}_{10}M_0 - K_R T \quad (1)$$

where M_0 is M extrapolated to $T = 0\%$. The slope is K_R , the retardation coefficient, which depends on gel fiber size and sample size:

$$\sqrt{K_R} = a \left(\sqrt{\pi l} \frac{D_{\text{eff}}}{2} + \sqrt{\pi l} r \right) \quad (2)$$

where a is a constant and l and r are the gel fiber length and radius. For spherical species, K_R increases with T , but for long polymer chains it decreases with T . This can result in either convex or concave Ferguson plots.^{22,23} To use eq 1 analysis is thus restricted to $T = 1.5\text{--}3.5\%$, the linear region following similar implementations in the literature.²⁴ To obtain values for K_R as a function of particle size, BPS functionalized Au particles of known size ($\langle D \rangle = 5.5\ \text{nm}$, $9.4\ \text{nm}$, $15\ \text{nm}$, $20\ \text{nm}$, Figure 2b) were analyzed as size

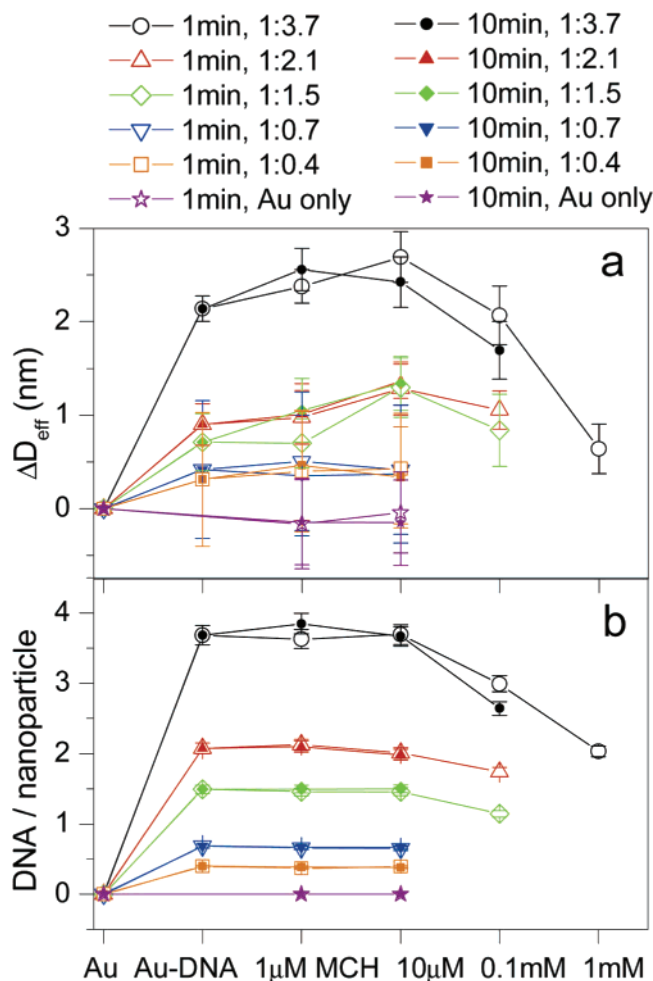


Figure 3. (a) ΔD_{eff} obtained for MCH of different reaction conditions as a function of MCH concentration for Au–DNA. Open symbols, 1 min reaction time; filled symbols, 10 min reaction time. Coverage ratio of Au–DNA before MCH treat is from 1:0.4 (squares), 1:0.7 (inverted triangles), 1:1.5 (diamonds), 1:2.1 (triangles), 1:3.7 (circles). ΔD_{eff} of plain Au particles (stars). (b) DNA per Au nanoparticle as a function of MCH treatment for different starting Au:DNA coverage ratios.

calibration standards. Since bigger particles are more retarded with increasing T , the slope of the Ferguson plot increases with Au size. These slopes are then utilized to obtain $\sqrt{K_R}$ of each nanoparticle size (eq 1) and fit to a linear dependence (Figure 2b, inset).²¹ For analysis of the Au–DNA samples, the obtained values of K_R are put into eq 1, and the Ferguson plots (Figure 2c) in combination with eq 2 yield D_{eff} of the samples.

Figure 3a shows the ΔD_{eff} , the difference between the diameter of Au–DNA and the diameter of the plain gold, obtained as a function of the MCH concentration (1 μM –1 mM) for a reaction time of 1 or 10 min. Only samples stable for at least a month after reaction with MCH are shown. ΔD_{eff} of Au/DNA of 1:3.7, 1 min curve (open circles), shows an initial increase upon functionalization with the oligo. With 10 μM MCH, D_{eff} increases additionally by 0.6 nm, indicating that the oligo adopts a slightly more radial configuration, increasing the effective size of the conjugate. At MCH concentrations ≥ 0.1 mM, the D_{eff} decreases to below the value of the Au–DNA conjugates. The reaction at high MCH

concentration was sometimes accompanied by particle aggregation, suggesting that the MCH completely displaced the DNA–SH and BPS. This shows that controlling the MCH concentration is key to obtaining the proper conformation of the oligo. For longer reaction times (10 min, filled circles) the behavior is similar to the 1 min reactions except at high concentrations (≥ 0.1 mM) D_{eff} approaches a smaller value. Au–DNA ratios after these MCH treatments are shown in Figure 3b as a function of MCH concentration. The coverage ratio is constant for MCH concentrations up to 10 μM but decreases ≥ 0.1 mM, illustrating that the DNA is not removed until this threshold value.

No significant size changes were observed from MCH reaction of plain Au particles (stars). MCH treatment was also repeated for Au/DNA ratios of 1:0.4 (squares), 0.7 (inverted triangles), 1.5 (diamonds), and 2.1 (triangles). An amount of 10 μM MCH still resulted in an increased D_{eff} for 2.1 and 1.5. For coverages $< 1:1$, no increase in D_{eff} was observed, probably due to the fact that there were not enough oligos on the particles to change hydrodynamic behavior in the gel regardless of conformation. Increased aggregation was also observed for concentrations ≥ 1 mM, making it unfeasible to obtain mobility information.

M_0 , the mobility at gel percentage of 0% (Figure 2c, inset), is a measure of the sample's charge²³ (as the DNA is not restricted by the pores of the gel). Its value is similar for all the Au and Au–DNA samples for MCH treatment of limited concentration and reaction time within the $\text{Log}_{10}M_0$ range of -3.50 to -3.48 . This indicates that the sample was not losing a considerable amount of DNA and BPS from the surface upon MCH treatment. However, for samples that have been exposed to MCH of high concentration, the M_0 decreases. This is consistent with a change in the charge of the species that occurs when DNA is displaced.

The capacity for forming a hybrid pair before and after MCH treatment was measured. Au–DNA conjugates were hybridized to a complementary strand modified with TAMRA (DNA-c, sequence in Table 1). Dehybridized DNA-c is no longer quenched due to the proximity of Au particles,^{12,18} and thus quantitation of TAMRA fluorescence provides a measure of the hybridization capacity of the DNA on the Au surface. Au–DNA conjugates with a coverage ratio 1:2.9 were used, and the ratio remained the same after the 10 μM /10 min MCH reaction, but decreased to 1:2.3 after the 0.1 mM/1 min MCH reaction. After MCH treatment, Au–DNA samples were adjusted to be at concentration of 5×10^{-8} M and DNA-c was in excess to enhance the hybridization (1×10^{-6} M), and the samples were annealed from 70 $^\circ\text{C}$ to 4 $^\circ\text{C}$ for about 30 min. Excess DNA-c was removed by gel electrophoresis. Figure 4 shows the number of dehybridized DNA-c per DNA-SH on the Au, defined as θ , as a function of temperature. Data were normalized to the temperature dependent fluorescent intensity of TAMRA. All samples show a sigmoidal step centered about 35 $^\circ\text{C}$, the T_m of the oligo confirmed by a melting curve of the plain DNA-SH–DNA-c hybrid under identical salt conditions. Both MCH treated samples show a higher capacity for DNA-c hybridized to the surface DNA than the non-MCH treated samples,^{16,17}

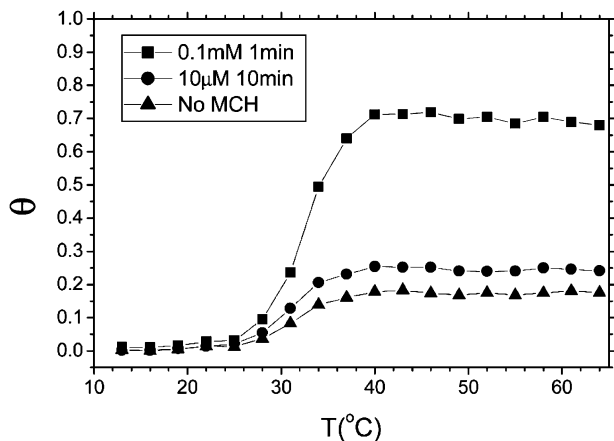


Figure 4. θ , the number of hybridized DNA-c per DNA-SH on the surface of the nanoparticle, as a function of temperature, obtained by fluorescence spectroscopy. Au–DNA without MCH reaction, triangles; with 10 μM /10 min MCH reaction, circles; and with 0.1 mM/1 min, squares.

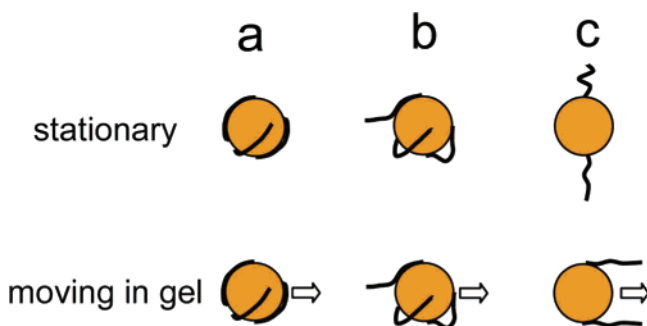


Figure 5. Illustration of Au–DNA conformation in gel when the samples are stationary or moving. Au–DNA without MCH, reaction (a); with 10 μM /10 min MCH, reaction (b); and with 0.1 mM/1 min MCH, reaction (c). Arrows indicate relative motion of the sample through a gel.

in which only <20% of the oligos are available for hybridization. The 0.1 mM MCH/1 min sample shows that $\sim 70\%$ of DNA-SH on the nanoparticle were hybridized with DNA-c, while the 10 μM /10 min sample shows only a nominal enhancement (25%) of hybridization over no MCH. Thus, it is believed that not all the adsorption sites were passivated by MCH in the 10 μM /10 min reaction.

Figure 5 illustrates possible hydrodynamic behavior induced by the change in DNA conformation. The contour length of a single-stranded 15mer is ~ 6.5 nm,²⁵ suggesting that the DNA is not completely straight on the nanoparticle surface even if the C6 linker were perfectly packed. This is expected based on estimates for the persistence length of single stranded DNA, which is 0.75–3 nm depending on salt conditions.^{25–27} Thus, the oligo would have at least a few bends. The 10 μM /10 min MCH reaction (b) has some oligo adsorption, resulting in an increased D_{eff} from the no-MCH sample (a). Due to this adsorption, its capacity for hybridization is minimally enhanced. In the case of the 0.1 mM/1 min reaction (c), the MCH covers enough of the particle surface such that the DNA does not adsorb. Although some of the DNA is displaced, it has an enhanced capacity for hybridization to a complement. The DNA-SH, which has

an inherently different mobility than Au nanoparticles, are not adsorbed to the surface and may have a tendency to align with the direction of motion during electrophoresis (“free draining”).²⁸ Consequently, this phenomenon results in a smaller measured D_{eff} . However, it should be noted that the behavior described in Figure 5 is only a hypothesis. It is difficult to predict the real conformation of Au–DNA with the type of (c) during the gel electrophoresis because hard spheres and polymer chains have very different electrophoretic properties.^{22,23,28}

In summary, MCH can be utilized on nanoparticle surfaces to control the conformation of covalently linked DNA oligos. Upon reaction with MCH, oligo adsorption to Au via bases is destabilized, changing the conformation of the oligo to one which is more amenable for hybridization. Control of both MCH concentration and reaction times are crucial for achieving the desired effect of oligo conformation change but not significant displacement from the nanoparticle surface. Further study is necessary to clearly reveal the electrophoretic behavior of the Au–DNA conjugate.

Experimental Details. (1) *Conjugation of Thiolated DNA Oligos to Au Nanoparticles.* Au nanoparticles with mean diameters 9.4 nm were obtained from Ted Pella in aqueous solutions stabilized by citrate or synthesized using literature methods.²⁹ The synthesis results in nanoparticles that are water soluble with size distributions of 10 nm \pm 1 nm, as quantified by TEM. The nanoparticle surfaces are then functionalized with bis(*p*-sulfonatophenyl) phenylphosphine dihydrate, dipotassium salt (BPS, Fluka, used as received), which has been determined to help keep the particles stable at high concentrations in aqueous solutions.¹⁹ The BPS-coated nanoparticles are precipitated from solution by addition of excess NaCl. These particles can then be resuspended into water at a higher concentration that is more amenable for visualization by gel electrophoresis. DNA oligonucleotides are purchased with C6 thiol group on the 5' end and a FAM on the 3' end (Proligo). The oligos were 15mers with a sequence as specified in Table 1, and purified by HPLC. Dithiol linkages between that result in oligo dimers were initially reduced by exposure to 50 mM dithiothreitol (DTT, Sigma Aldrich, used as received) for 1 day prior to reaction with the Au nanoparticles. Excess DTT is removed by extraction into ethyl acetate (EM Science, used as received) at $\geq 3\times$ the volume of the aqueous fraction multiple times (>3), which dissolves DTT but not the DNA, which is charged and more hydrophilic. Conjugation is done in increasing salt concentration by lyophilizing the solution, which is found to help conjugation by increasing screening of the DNA–DNA or DNA–Au electrostatic repulsion. Nanoparticle–oligo conjugates were resuspended in buffer $0.5\times$ TBE.

(2) *MCH Treatment of DNA–Nanoparticle Conjugates.* MCH was purchased from Sigma Aldrich and used as received.

(3) *Gel Electrophoresis.* Gel electrophoresis is done in agarose gels of varying percentages in $0.5\times$ TBE. Agarose was obtained from Invitrogen, TBE from EMD Chemicals Inc., and were used as received. Running buffer is $0.5\times$ TBE.

Samples were at a concentration of 1×10^{-7} M. Electric field strengths were fixed at 3.87 V/cm and total running times were measured (approximately 2 h for each gel). Gel percentage ranged from 1.5 to 3.5 wt %/volume. At least four data points were used to fit to eq 1 for each sample.

(4) *Fluorescence Spectroscopy*. Fluorescence spectroscopy was performed on a Spex Fluoromax 3. FAM fluorescence was performed with $\lambda_{\text{excitation}} = 495$ nm and $\lambda_{\text{emission}} = 515$ nm. TAMRA fluorescence was performed with an $\lambda_{\text{excitation}} = 555$ nm and $\lambda_{\text{emission}} = 580$ nm. Temperature control was via a Peltier module.

Acknowledgment. S.P. was supported by the National Science Foundation (NSF CCR-0122419). K.A.B. was supported by the James H. Ferry Fund.

References

- (1) Xiao, S.; Liu, F.; Rosen, A. E.; Hainfeld, J. F.; Seeman, N. C.; Musier-Forsyth, K.; Kiehl, R. A. *J. Nanoparticle Res.* **2002**, *4*, 313–317.
- (2) Taton, T. A.; Mirkin, C. A.; Letsinger, R. L. *Science* **2000**, *289*, 1757–1760.
- (3) Niemeyer, C. M. *Angew. Chem., Int. Ed. Engl.* **2001**, *40*, 4128–4158.
- (4) Hamad-Schifferli, K.; Schwartz, J. J.; Santos, A. T.; Zhang, S.; Jacobson, J. M. *Nature* **2002**, *415*, 152–155.
- (5) Loweth, C. J.; Caldwell, W. B.; Peng, X.; Alivisatos, A. P.; Schultz, P. G. *Angew. Chem., Int. Ed. Engl.* **1999**, *38*, 1808–1812.
- (6) Storhoff, J. J.; Elghanian, R.; Mirkin, C. A.; Letsinger, R. L. *Langmuir* **2002**, *18*, 6666–6670.
- (7) Parak, W. J.; Pellegrino, T.; Micheel, C. M.; Gerion, D.; Williams, S. C.; Alivisatos, A. P. *Nano Lett.* **2003**, *3*, 33–36.
- (8) Josephson, L.; Perez, J. M.; Weissleder, R. *Angew. Chem., Int. Ed. Engl.* **2001**, *40*, 3204–3206.
- (9) Westin, L.; Xu, X.; Miller, C.; Wang, L.; Edman, C. F.; Nerenberg, M. *Nat. Biotechnol.* **2000**, *18*, 199–204.
- (10) Park, S.-J.; Taton, T. A.; Mirkin, C. A. *Science* **2002**, *295*, 1503–1506.
- (11) Zanchet, D.; Micheel, C. M.; Parak, W. J.; Gerion, D.; Williams, S. C.; Alivisatos, A. P. *J. Phys. Chem. B* **2002**, *106*, 11758–11763.
- (12) Dubertret, B.; Calame, M.; Libchaber, A. *Nat. Biotechnol.* **2001**, *19*, 365–370.
- (13) Nelson, B. P.; Grimsrud, T. E.; Liles, M. R.; Goodman, R. M.; Corn, R. M. *Anal. Chem.* **2001**, *73*, 1–7.
- (14) Pease, A. C.; Solas, D.; Sullivan, E. J.; Cronin, M. T.; Holmes, C. P.; Fodor, S. P. A. *Proc. Natl. Acad. Sci. U.S.A.* **1994**, *91*, 5022–5026.
- (15) Kelley, S. O.; Barton, J. K.; Jackson, N. M.; McPherson, L. D.; Potter, A. B.; Spain, E. M.; Allen, M. J.; Hill, M. G. *Langmuir* **1998**, *14*, 6781–6784.
- (16) Herne, T. M.; Tarlov, M. J. *J. Am. Chem. Soc.* **1997**, *119*, 8916–8920.
- (17) Mbindyo, J. K. N.; Reiss, B. D.; Martin, B. R.; Keating, C. D.; Natan, M. J.; Mallouk, T. E. *Adv. Mater.* **2001**, *13*, 249–254.
- (18) Demers, L. M.; Mirkin, C. A.; Mucic, R. C.; Reynolds, R. A., III.; Letsinger, R. L.; Elghanian, R.; Viswanadham, G. *Anal. Chem.* **2000**, *72*, 5535–5541.
- (19) Zanchet, D.; Micheel, C. M.; Parak, W. J.; Gerion, D.; Alivisatos, A. P. *Nano Lett.* **2001**, *1*, 32–35.
- (20) Wang, S.; Mamedova, N.; Kotov, N. A.; Chen, W.; Studer, J. *Nano Lett.* **2002**, *2*, 817–822.
- (21) Rodbard, D.; Chrambach, A. *Proc. Natl. Acad. Sci. U.S.A.* **1970**, *65*, 970–977.
- (22) Serwer, P. *Electrophoresis* **1989**, *10*, 327–331.
- (23) Tietz, D.; Chrambach, A. *Electrophoresis* **1986**, *7*, 241–250.
- (24) Griess, G. A.; Moreno, E. T.; Easom, R. A.; Serwer, P. *Biopolymers* **1989**, *28*, 1475–1484.
- (25) Tinland, B.; Pluen, A.; Sturm, J.; Weill, G. *Macromolecules* **1997**, *30*, 5763–5765.
- (26) Goddard, N. L.; Bonnet, G.; Krichevsky, O.; Libchaber, A. *Phys. Rev. Lett.* **2000**, *85*, 2400–2403.
- (27) Smith, S. B.; Cui, Y.; Bustamante, C. *Science* **1996**, *271*, 795–799.
- (28) Viovy, J.-L. *Rev. Mod. Phys.* **2000**, *72*, 813–872.
- (29) Jana, N. R.; Peng, X. *J. Am. Chem. Soc.* **2003**, *125*, 14280–14281.

NL048920T